

$$\Delta v = 1 - \frac{\cos(\beta + \phi)}{\cos(\phi)}$$

with:

β : (positive) phase shift due to internal impedance

ϕ : load angle (positive with lagging load current)

In case of two series connected PSTs the total voltage drop Δv_2 is:

$$\Delta v_2 = 1 - (1 - \Delta v)^2$$

Assuming a standard operating condition with p.f. = 0,96 lagging and choosing a maximum impedance voltage $z = 11\%$, a 7,3% voltage drop is obtained. This choice is a good compromise between PST short circuit withstand capability and network power quality.

The PST winding arrangement is shown in Fig. 2 along with its phasor diagram.

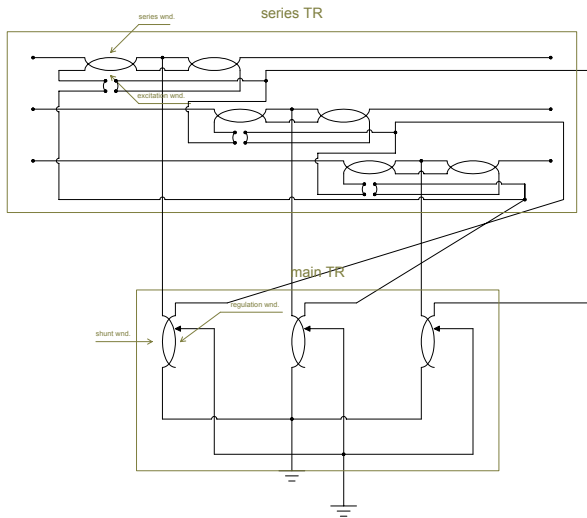


Fig. 2 Symmetric, quadrature type, dual core PST winding arrangement

The main PSTs characteristics are summarized in Table I.

TABLE I MAIN PSTS CHARACTERISTICS

Rated power	1800MVA
Rated frequency	50 Hz
Rated voltage	400 kV
Maximum no-load angle	$\pm 17,5^\circ$
Maximum impedance voltage at maximum angle	11%

The adopted scheme includes the possibility to by-pass the two PSTs. The scheme of PST connection to the 400 kV network is shown in Fig. 3.

400 kV busbars

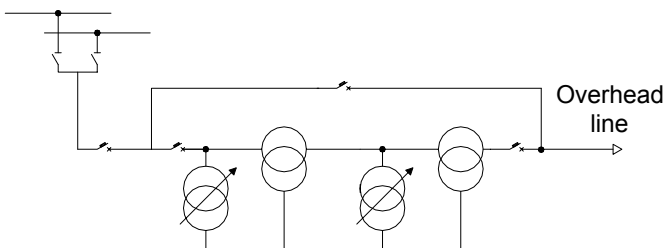


Fig. 3 simplified single line diagram of PST connection to the 400 kV network (several disconnectors and instrument transformers are not shown)

III. DESCRIPTION OF THE PST MODEL AND CALCULATION OF ITS PARAMETERS

In the following the SCFTRAN model is briefly recalled, a comprehensive description has been written by the model developer in [1]. The model is based on finite sectioning of transformer core with lumped non-linear circuit elements, that are obtained on the basis of duality between magnetic and electric circuits. Being the model based on physical quantities, windings and core geometry has to be known or estimated with sufficient accuracy. In the case dealt within this paper, the PST geometry has been obtained on the basis of some manufacturers data while some others parameters have been calculated/estimated.

A. Linear impedances modeling

The linear portion of the transformer is modeled in SCFTRAN by means of a linear array. The linear impedances have been calculated by means of Finite element method analysis that has been carried out with the FEMM software [3]. For air core self-inductances calculation 2D axisymmetric analysis has been applied. An example of air-core inductance calculated with FEM is shown in Fig. 4.

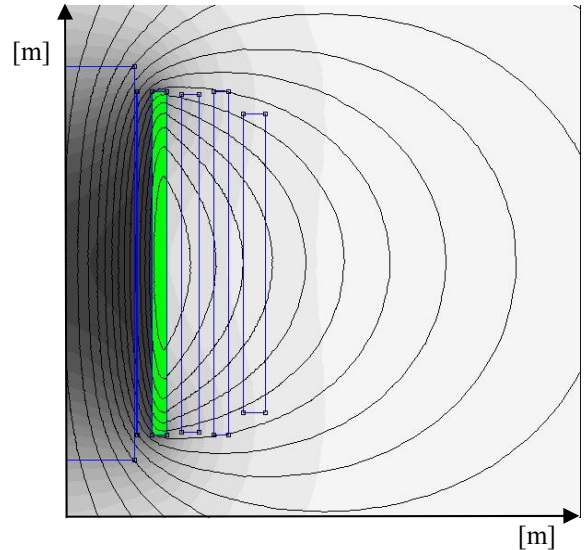


Fig. 4. FEM air-core calculation of magnetic flux density in the PST exciting unit

B. Magnetic circuit modeling

As shown in [1] reluctances \mathfrak{R} and loss elements \mathfrak{L} are used to model accurately the Watt losses and MMF drops in magnetic core; their value is calculated as:

$$\mathfrak{R} = \frac{\text{flux}_{\text{path}_{\text{length}}}}{\mu_0 \mu_r \text{CROSS}_{\text{section}_{\text{area}}}}; \quad \mathfrak{L} = \frac{\text{Watt}_{\text{losses}}}{\left(\frac{d\Phi}{dt}\right)^2}$$

Magnetic circuit is solved in the electric domain by means of ATP; the core equivalent electric circuit preserve recognizable topology and allows use of non-linear elements present in ATP libraries.

Any magnetic element is related to its electrical equivalent by a standard number of turns (i.e.100 in [1]):

$$L = \frac{N^2}{\mathfrak{R}}; \quad R = \frac{\mathfrak{L}}{N^2}$$

Fluxes and MMFs can be converted in terms of voltages and currents with the following familiar relationships:

$$I_{coil} = \frac{MMF}{N}; \quad V_{coil} = N \frac{d\phi}{dt}$$

Every flux path is thus represented in the electric domain with a ladder non-linear circuit, whose elements are strictly linked to geometrical and physical data of the path itself. Fig. 5 [1] shows how to represent any core element.

Residual MMF and hysteresis, whose importance is paramount in energization studies, is also modeled via TACS-controlled current sources.

Further details about this method can be read in [1]. Because of its accuracy such a method requires several realistic input data, as B-H curve for both core and tank steel, geometrical parameters of core, windings and tank, etc.

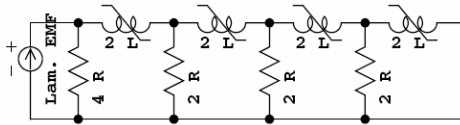


Fig. 5. Core element finite section representation [1]

AC magnetization curve of the laminated steel (Fig. 6) has been used as B-H characteristics to feed non-linear ATP elements. The no-load PST losses have been estimated to be made up of 50% of hysteresis losses and 50% of eddy current losses. The final model make use of 8 finite sections elements to model lamination for any component of the core. Also flux shields, tank walls and tank top have been represented with their actual dimension and a suitable B-H curve.

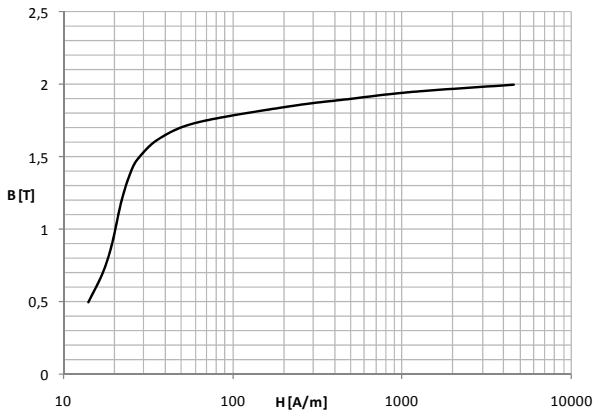


Fig. 6. AC magnetization curve of the modeled magnetic core steel

IV. DESCRIPTION OF THE STUDIED SYSTEM

The studied 400kV portion of the Italian transmission grid is shown in Fig. 7.

All the 400 kV transmission lines have been simulated with the constant parameter distributed line (Bergeron) model. The 400 kV network has been considered at no-load with a short circuit power of the equivalent generators corresponding to the minimum load dispatching values.

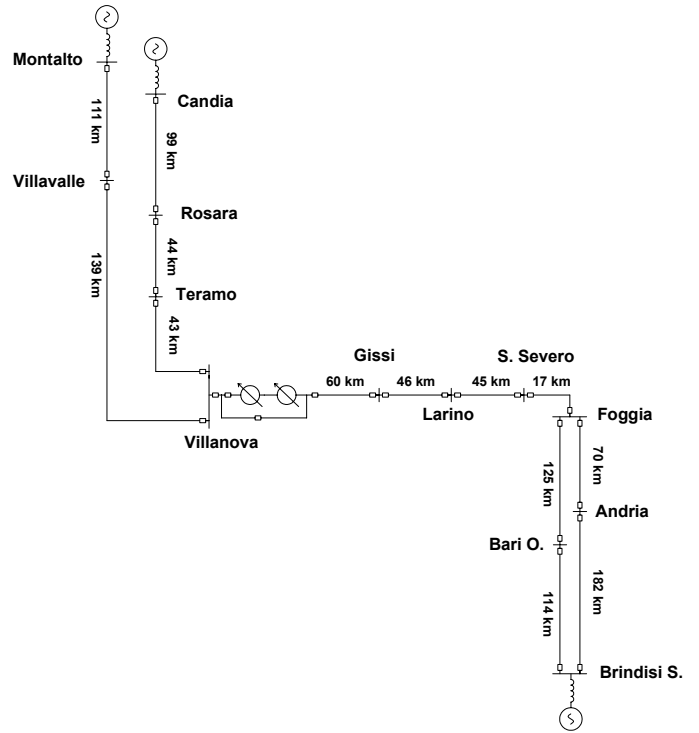


Fig. 7. The studied 400kV portion of the Italian transmission grid

V. TIME DOMAIN STUDY

In the following the SCFTRAN model is briefly recalled, a comprehensive description has been written by the model

A. PST no-load energization

As the instant of circuit breaker closure with reference to voltage sinewave plays a major role in determining inrush current peak value, a statistic study has been carried-out.

In the study, based on 1000 simulations, network short circuit power has been assumed to be 6800MVA. Line-to-line voltage has been set to 400kV.

The cumulative probability distribution found with the statistic study is shown in Fig. 8 for the PST with and without residual flux, while a typical PST inrush transient simulated with the described model in the ATP-EMTP is shown in Fig. 9.

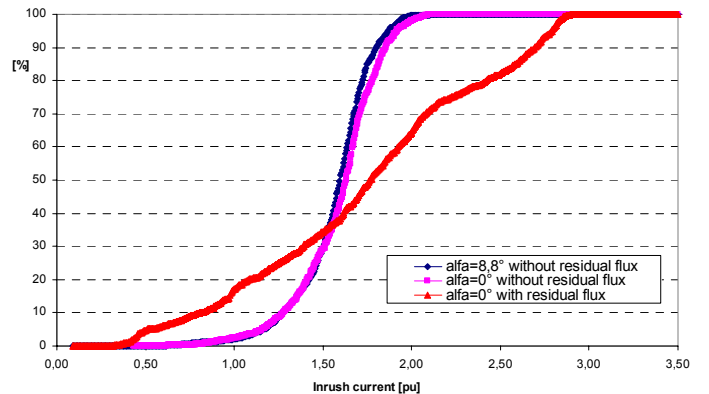


Fig. 8. Cumulative probability distribution of the PST peak inrush current (without synchronized switching)

The model is expected to properly reproduce the harmonic content in the inrush current and is therefore suitable also for protection relays studies.

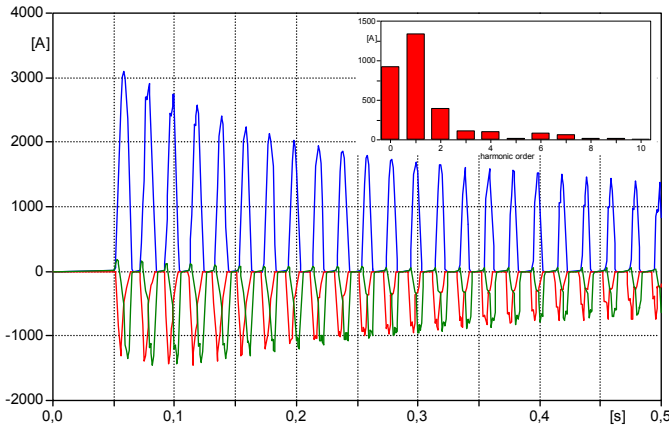


Fig. 9. Phase currents of a typical PST inrush transient simulated with the described model in the ATP-EMTP. Fourier analysis of the phase c (blue) is shown (time window: $0.08s \div 0.1s$)

The maximum inrush current is $2450 A_{\text{peak}}$ without considering residual flux while it is $3250 A_{\text{peak}}$ taking into account the residual flux. This value is lower than the rated current of the PST, although while in the normal operation all the current flows in the series unit, having a rated current of $2598 A_{\text{RMS}}$, during the inrush all the current flows in the excitation winding, that has a rated current of $793 A_{\text{RMS}}$.

Being a large rated power transformer, compared with the short circuit power of the network, the inrush transient in the most unfavorable conditions (network conditions, and circuit breaker closure times) entails a significant voltage drop (up to 15%) due to reactive power absorption and a possible risk of low-order harmonic resonances along with temporary overvoltages could not be excluded.

The use of synchronized switching of the PST circuit breakers has therefore been required in order to minimize the inrush transients and the consequent mechanical stress on the exciting unit of the PST.

B. No-load energization of the 400kV line connected in series with the PSTs

A statistic study, based on 1000 simulations, has been carried out to calculate the maximum switching overvoltages during the energization of the 400kV line connected in series to the PST.

The cumulative probability distribution found with the statistic study is shown in Fig. 10 for the overhead line energization with and without the PST. Even with the PST the maximum switching overvoltages are tolerable as they are much lower than the switching impulse test voltage for the PSTs (1050 kV, i.e. about 3.1 p.u.) and of the overhead line SIWV that is about 3.0 p.u. for Italian 400 kV lines.

Moreover PSTs will be protected at both terminals by means of surge arresters with a SIPL of 2.1 p.u.

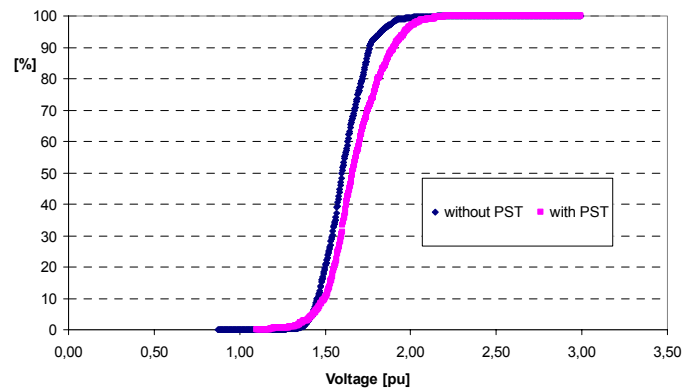


Fig. 10. Cumulative probability distribution of the 400kV receiving end voltage during its energization with and without the PSTs

C. By-pass CB closure transient

The by-pass closure is a maneuver that can entail high currents circulating in the PST/by-pass loop. The amplitude of these currents increases with the phase shift of the PST prior to by-pass closure.

The by-pass closure has been simulated with the PSTs at no-load with $\alpha_0=8,83^\circ$ (i.e. half the regulating range). In this case the phase currents can reach the peak value of 12kA, as shown in Fig.11 and a corresponding reactive power absorption of about 820MVAR.

The maximum expected current peak value during by-pass closure with $\alpha_0=17^\circ$ is about 20kA with the PST at no-load. This current value entails both mechanical stress on the PSTs and high reactive power absorption (up to 1000MVAR) with consequent unacceptable voltage drop at the 400kV busbars. It is therefore necessary to allow the PST by-passing only after having set the phase angle as close as possible to the “zero equivalent” position, as defined in the following section.

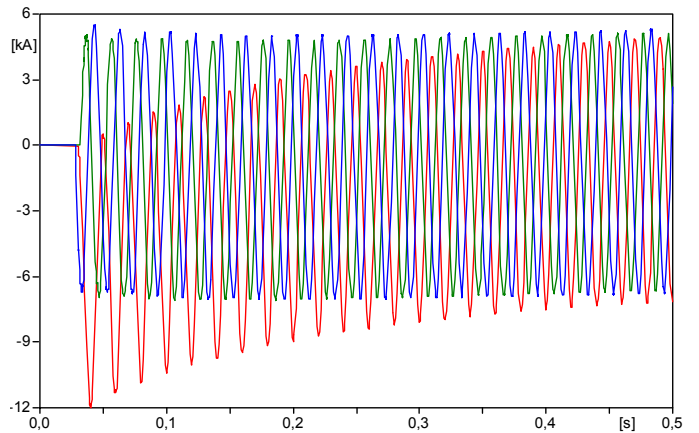


Fig. 11. Phase currents in the PST by-pass during by-pass CB closure ($\alpha=8,83^\circ$)

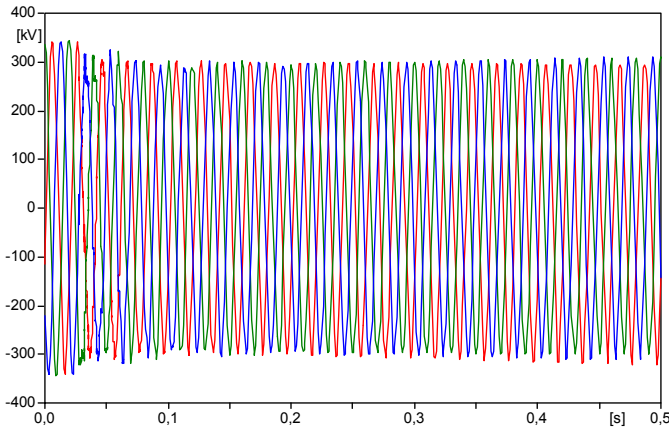


Fig. 12. Phase voltages at the PST terminals during by-pass CB closure ($\alpha=8,83^\circ$)

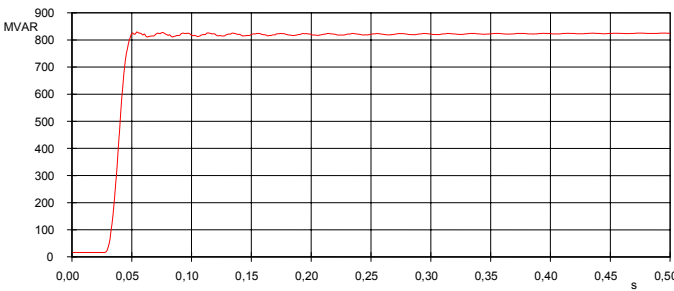


Fig. 13. Reactive power absorbed by the PST during by-pass CB closure ($\alpha=8,83^\circ$)

VI. ZERO EQUIVALENT CALCULATION AND BY-PASS OPERATION

In a symmetric PST on load phase shift α (see Fig. 1) is given by the difference between the no-load phase shift α_0 and the phase shift due to the PST internal impedance β :

$$\alpha = \alpha_0 - \beta$$

The no-load phase shift α_0 must be taken as positive in boost mode and negative in buck mode.

With reference to Fig.1, assuming the rated voltage at source side and a purely reactive PST internal impedance, the phase shift β is given by:

$$\beta = \arcsin(z \cdot \gamma \cdot \cos \phi)$$

With:

z being the per unit impedance voltage of the PST

γ the load factor (ratio between the load current and rated current).

The by-pass is used during the PST connection and disconnection maneuvers to avoid the line interruption.

In other cases it could be convenient to put in operation the line with the PST already connected, in this way the phase shift between the two line terminals can be compensated. This could be useful in case of a line connecting two networks with high phase shift.

With the by-pass closed the line current is shared among the two branches as shown in Fig 14:

$$I_1 = I_2 + I_3$$

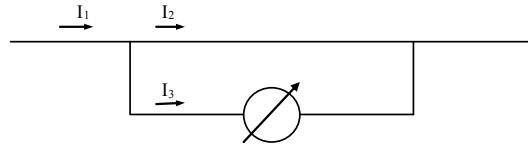


Fig. 14. Currents sharing between the PST and the closed by-pass

After PST connection, the by-pass sets the phase shift at PST terminal to zero.

$$\alpha = 0 \rightarrow \beta = \alpha_0$$

The amplitude and sign of I_3 must therefore yield a β that satisfies the above condition.

To minimize the transient following the by-pass opening, the amplitude I_2 has to be close to zero.

$$I_2 \cong 0 \rightarrow I_1 \cong I_3$$

This means that all the line current has to flow in the PST branch; i.e. there is no current circulating in the PST/by-pass loop. Such loop current would require a reactive power absorption, being the loop an inductive circuit.

The required condition is attained choosing an α_0 in boost mode that compensate a β , calculated setting the PST current equal to the line current. Assuming the operating voltage equal to the rated value this condition is straightforwardly expressed with the following formula:

$$P = \sin \alpha_0 \cdot \frac{U_r^2}{Z}$$

P being the active power flowing in the line before the PST connection

Z being the PST internal impedance [in ohm] at the selected α_0

Similar considerations can be done for the by-pass closure during PST operation. In this case the zero equivalent condition minimizes the phase shift due to the PST, thus the by-pass closing does not change the line active power and the reactive power absorbed by the PST.

VII. CONCLUSIONS

The used model [1] is suitable to model transients up to few kHz and takes into account residual flux, hysteresis and EM field propagation through the core.

The PST inrush current statistical study, carried out taking into account the residual flux showed the need to use synchronized switching of PSTs CB. With this solution the energization transient can be minimized with the following benefits:

- reduction of mechanical stress in the exciting unit
- reduction of the voltage variation in the network during PST energization
- reduction of risk of resonance excitation and corresponding temporary overvoltages

The switching overvoltages during the energization of the 400kV line connected in series with the PST are in line with the usual expected values in the Italian transmission network (i.e. below 2.7 p.u.).

The PSTs CB by-pass closure yields high currents in the PSTs. Their amount increases with the phase shift of the PST prior to by-pass closure and can reach the peak value of 20 kA.

This current value entails both mechanical stress of the PSTs and high reactive power absorption (up to 1000MVAR) with consequent unacceptable voltage drop at the 400kV busbars. It is therefore necessary to allow the PST by-passing only after having set the phase angle as close as possible to the “zero equivalent” position.

VIII. REFERENCES

- [1] Robert J. Meredith (2008, June 23). *Atp modeling of core-form transformers by magnetic circuit analysis, including finite sectioning*. (2nd ed.), [Online].
- [2] L. Colla, V. Iuliani, F. Palone, M. Rebolini, C. Taricone " EHV/HV autotransformers modeling for electromagnetic transients simulation of power systems," in *Proc. 2010 IEEE Industrial Electronics Society International Conf. on Electrical Machines*, paper RF-010855.
- [3] David Meeker, Finite Element Method Magnetics V.4.2 Feb.2009